

# Determination of Molecular Orientation in Biaxially Oriented Ultrathin Films

Isabelle Pelletier,<sup>†,‡</sup> Isabelle Laurin,<sup>†</sup> Thierry Buffeteau,<sup>§</sup> and Michel Pérozet\*,<sup>†</sup>

Centre de Recherche en Science et Ingénierie des Macromolécules, Département de Chimie, Université Laval, Québec, Qc, G1K 7P4, Canada, and Laboratoire de Physico-Chimie Moléculaire, UMR 5803 du CNRS, Université Bordeaux I, 33405 Talence, France.

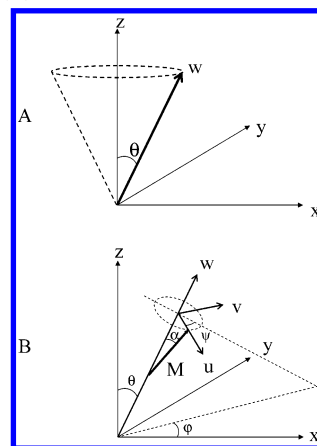
Received: July 29, 2003; In Final Form: February 24, 2004

Biaxial orientation in ultrathin films is characterized by a preferential orientation of the main molecular axis in the plane of the film in addition to its orientation with respect to the normal of the film. In this paper, analytical expressions allowing the calculation of the molecular orientation in biaxially oriented films from their anisotropic optical constants are presented for the first time. These expressions have been used to calculate the molecular orientation in multilayers of poly( $\gamma$ -benzyl-L-glutamate) and to determine the angles between the main molecular axis and the different transition moments used ( $\alpha$  angles). Using the optical constants determined by Buffeteau et al.<sup>1</sup> for PBG multilayers, we have found that the tilt angle of the PBG helices with respect to the monolayer normal is  $89^\circ$  and that the azimuthal angle in the plane is  $57^\circ$ . The calculated  $\alpha$  angles for the carbonyl stretching mode of the ester group and the amide I and amide II modes of the amide group are  $49^\circ$ ,  $34^\circ$  and  $74^\circ$ , respectively. The analytical expressions presented in this paper have also been used to calculate the molecular orientation in Langmuir–Blodgett monolayers of an equimolar blend of poly(D-lactide) and poly(L-lactide). The optical constants of a monolayer of the polylactide mixture determined using p- and s-polarized transmittance and p-polarized reflection–absorption infrared spectra have shown that the polylactide helices have a tilt angle of  $81^\circ$  and an azimuthal angle of  $56^\circ$ .

## Introduction

Ultrathin films have received considerable attention for many years because of their wide range of potential applications as sensors,<sup>2,3</sup> lubricants,<sup>4</sup> or electronic devices.<sup>5,6</sup> Recently, the study of molecular orientation in these films has received a considerable amount of attention because of its relationship to the film structure and surface functionality. The Langmuir–Blodgett (LB) deposition has always been one of the most useful techniques to prepare ultrathin films. Usually, the spontaneous orientation of molecules at the air/water interface causes Langmuir films to adopt a uniaxial orientation. This type of orientation is shown in Scheme 1A, where the main molecular axis,  $w$ , makes a tilt angle ( $\theta$ ) with respect to the normal of the film ( $z$ ), but has no preferential orientation in the plane of the film ( $x, y$  plane). Recently, biaxial orientation has been observed in LB films of various compounds transferred onto solid substrates.<sup>1,7–10</sup> This more complex type of orientation, shown in Scheme 1B, is characterized by a preferential orientation of the main molecular axis in the plane of the film (expressed by the azimuthal angle  $\varphi$ ) in addition to its orientation with respect to the normal of the film (expressed by the tilt angle  $\theta$ ). This type of orientation has been mainly reported for macromolecules with a rodlike shape, such as helices. Most of the time, the in-plane orientation is introduced by the LB transfer of these films, while their out-of-plane orientation is already present at the air/water interface. It has been proposed that the molecular

**SCHEME 1:** Space Coordinate System ( $x, y, z$ ), Molecular Coordinate System ( $u, v, w$ ), Transition Moment ( $M$ ), and the Different Angles Used to Describe the Molecular Orientation for Films Showing (A) Uniaxial and (B) Biaxial Orientations



reorientation occurring during the LB deposition is due to convection flows induced in the monolayer by the transfer.<sup>11–14</sup>

Infrared spectroscopy is a particularly useful technique to study the molecular orientation in ultrathin films because it can provide information about films either on solid substrates or at the air/water interface. Several approaches have been developed to calculate the molecular orientation in ultrathin films from their infrared spectra. These methods, utilizing polarized attenuated total reflectance (ATR), reflectance at grazing incidence (IRRAS), and transmittance spectra either alone or in combination, are usually not suited to the study of biaxially oriented films.<sup>15–27</sup> The only methods that can be applied to the study

\* To whom correspondence should be addressed. E-mail: michel.perozet@chm.ulaval.ca. Fax: (418)656-7916.

<sup>†</sup> Université Laval.

<sup>‡</sup> Present address: Department of Materials Science and Engineering, University of Delaware, Newark, Delaware 19716.

<sup>§</sup> Université Bordeaux I.

of such films are generally limited to the use of bands having their transition moment perpendicular or parallel to the main molecular axis.<sup>28–33</sup>

The most promising method for studying the molecular orientation in biaxially oriented films has recently been introduced by Buffeteau et al.<sup>34</sup> This method, which uses the anisotropic optical constants of a film to calculate its molecular orientation, has already been applied to the study of different ultrathin films.<sup>1,34–39</sup> All of these films presented a uniaxial orientation, except the poly( $\gamma$ -benzyl-L-glutamate) (PBG) multilayered film that showed a biaxial orientation.<sup>1,38</sup> For the former films, the optical constants were determined and then used to calculate the molecular orientation (i.e., the tilt angle,  $\theta$ ) using the well-known equations proposed by Fraser and McRae.<sup>40</sup> For the PBG film, the optical constants were also determined, but the Fraser and McRae equations could not be used because they require a uniaxial orientation. The molecular orientation had to be calculated assuming that the PBG helices were lying perfectly in the plane of the film ( $\theta = 90^\circ$ ), leading to the calculation of the azimuthal angle,  $\varphi$ , alone. Obviously, such an assumption cannot be made for all biaxially oriented films. There is thus a significant need to generalize the Fraser and McRae equations (i.e., to derive analytical expressions allowing the calculation of the molecular orientation in biaxially oriented films from their optical constants).

In this paper, such analytical expressions linking the molecular tilt and azimuthal angles ( $\theta$  and  $\varphi$ ) to the anisotropic optical constants of a film are presented for the first time. These equations have been derived by considering that the molecules do not have any preferential orientation around their main axis (cylindrical symmetry). The validity of these equations has been verified by calculating the molecular orientation in PBG multilayers. The molecular orientation so calculated has been compared to that previously obtained by Buffeteau et al.<sup>1</sup> and Takenaka et al.<sup>28</sup> These new equations have also been used to study a LB monolayer of an equimolar blend of poly(D-lactide) and poly(L-lactide) for which the anisotropic optical constants have been determined in this paper. Results show that the polylactide helices display a biaxial orientation but that the transition moments associated with most of their vibrations do not display cylindrical symmetry. Although the expressions presented here are in principle not applicable to this case, they can be used for vibrations having their transition moments parallel to the main molecular axis because the transition moment of such a vibration has intrinsic cylindrical symmetry.

## Theory

The biaxial orientation of a transition moment ( $M$ ) can be described with respect to the space coordinate system by using the Euler angles as shown in Scheme 1B. The space coordinate system is formed by the  $x$ ,  $y$ , and  $z$  axes, where  $x$  and  $y$  define the plane of the film and  $z$  is normal to the film. The  $u$ ,  $v$ , and  $w$  axes form the molecular coordinate system in which  $w$  is the main axis of the molecule. The orientation of this axis with respect to the space coordinate system is described by the two first Euler angles, the tilt ( $\theta$ ) and azimuthal ( $\varphi$ ) angles, and the orientation of a transition moment with respect to main molecular axis ( $w$ ) is defined by the  $\alpha$  angle and by the third Euler angle, the twist angle ( $\psi$ ).

Zbinden<sup>41</sup> has shown that the components of the transition dipole moment along each axis in the space coordinate system ( $M_x$ ,  $M_y$ , and  $M_z$ ) can be expressed as functions of the three Euler angles and of the components of the transition dipole moment along the axis of the molecular coordinate system

( $M_u$ ,  $M_v$ , and  $M_w$ ) as follows:

$$\begin{pmatrix} M_x \\ M_y \\ M_z \end{pmatrix} = \begin{pmatrix} \cos \psi \cos \theta \cos \varphi + \sin \psi \sin \varphi & \sin \psi \cos \theta \cos \varphi - \cos \psi \sin \varphi & \cos \varphi \sin \theta \\ \cos \psi \cos \theta \sin \varphi - \sin \psi \cos \varphi & \sin \psi \cos \theta \sin \varphi + \cos \psi \cos \varphi & \sin \varphi \sin \theta \\ -\sin \theta \cos \psi & -\sin \theta \sin \psi & \cos \theta \end{pmatrix} \begin{pmatrix} M_u \\ M_v \\ M_w \end{pmatrix} \quad (1)$$

Using the system of axes defined in Scheme 1B, the transition dipole moment along the axes of the molecular coordinate system can be easily expressed as functions of the absolute magnitude of the transition dipole moment  $M$  and of the  $\alpha$  angle by the relations

$$M_u = M \sin \alpha \quad M_v = 0 \quad M_w = M \cos \alpha \quad (2)$$

Inserting these relations into eq 1, we can write the components of the transition dipole moment along each axis of the space coordinate system as

$$M_x = (\cos \psi \cos \theta \cos \varphi + \sin \psi \sin \varphi) \cdot M \sin \alpha + \cos \varphi \sin \theta \cdot M \cos \alpha \quad (3)$$

$$M_y = (\cos \psi \cos \theta \sin \varphi - \sin \psi \cos \varphi) \cdot M \sin \alpha + \sin \varphi \sin \theta \cdot M \cos \alpha \quad (4)$$

$$M_z = -\sin \theta \cos \psi \cdot M \sin \alpha + \cos \theta \cdot M \cos \alpha \quad (5)$$

Considering that the extinction coefficients along each axis of the space coordinate system are proportional to the square of the transition dipole moment ( $k_x = KM_x^2$ ,  $k_y = KM_y^2$ , and  $k_z = KM_z^2$ , where  $K$  is a constant of proportionality), we obtain

$$k_x = k_{\max} [\cos \psi \cos \theta \cos \varphi \sin \alpha + \sin \psi \sin \varphi \sin \alpha + \cos \varphi \sin \theta \cos \alpha]^2 \quad (6)$$

$$k_y = k_{\max} [\cos \psi \cos \theta \sin \varphi \sin \alpha - \sin \psi \cos \varphi \sin \alpha + \sin \varphi \sin \theta \cos \alpha]^2 \quad (7)$$

$$k_z = k_{\max} [-\sin \theta \cos \psi \sin \alpha + \cos \theta \cos \alpha]^2 \quad (8)$$

where  $k_{\max} = KM$  is the maximum extinction coefficient, which is given for each wavenumber by the sum of  $k_x$ ,  $k_y$ , and  $k_z$ .

Finally, assuming a cylindrical symmetry of the transition dipole moment with respect to the main molecular axis (integration of  $k_x$ ,  $k_y$ , and  $k_z$  over the  $\psi$  angle), we easily obtain the expression of the extinction coefficients in the space coordinate system:

$$k_x = k_{\max} \left[ \frac{1}{2} \cos^2 \theta \cos^2 \varphi \sin^2 \alpha + \frac{1}{2} \sin^2 \varphi \sin^2 \alpha + \cos^2 \varphi \sin^2 \theta \cos^2 \alpha \right] \quad (9)$$

$$k_y = k_{\max} \left[ \frac{1}{2} \cos^2 \theta \sin^2 \varphi \sin^2 \alpha + \frac{1}{2} \cos^2 \varphi \sin^2 \alpha + \sin^2 \varphi \sin^2 \theta \cos^2 \alpha \right] \quad (10)$$

$$k_z = k_{\max} \left[ \frac{1}{2} \sin^2 \theta \sin^2 \alpha + \cos^2 \theta \cos^2 \alpha \right] \quad (11)$$

Although eqs 9–11 are fully functional, it is more convenient

to express them as functions of the orientation parameters,  $f_\theta$  and  $f_\varphi$ , introduced by Stein<sup>42,43</sup> to express orientation in biaxially oriented films:

$$f_\theta = \left(\frac{1}{2}\right)(3\langle\cos^2\theta\rangle - 1) \quad (12)$$

$$f_\varphi = 2\langle\cos^2\varphi\rangle - 1 \quad (13)$$

where  $\langle\cos^2\theta\rangle$  and  $\langle\cos^2\varphi\rangle$  are the mean values of  $\cos^2\theta$  and  $\cos^2\varphi$  for a distribution of transition moments in the film. Equations 9–11 can thus be rewritten in terms of these orientation parameters as follows:

$$k_x = k_{\max} \left[ \left( \left( \frac{1}{2} \right) \sin^2\alpha - \left( \frac{1}{3} \right) \right) (f_\theta + f_\theta f_\varphi - f_\varphi) + \left( \frac{1}{3} \right) \right] \quad (14)$$

$$k_y = k_{\max} \left[ \left( \left( \frac{1}{2} \right) \sin^2\alpha - \left( \frac{1}{3} \right) \right) (f_\theta - f_\theta f_\varphi + f_\varphi) + \left( \frac{1}{3} \right) \right] \quad (15)$$

$$k_z = k_{\max} \left[ \left( \cos^2\alpha - \left( \frac{1}{3} \right) \right) f_\theta + \left( \frac{1}{3} \right) \right] \quad (16)$$

Equations 9–11 and, therefore, eqs 14–16 link the molecular orientation in a film ( $\theta$  and  $\varphi$ ) to the extinction coefficients ( $k_x$ ,  $k_y$ , and  $k_z$ ) and to the  $\alpha$  angle between the transition moment considered and the main molecular axis. They are equivalent to the Fraser and McRae equations, but they allow the calculation of the molecular orientation of biaxially oriented films from the optical constants without the use of any assumptions regarding the molecular orientation. Moreover, when applied to the simultaneous study of many vibrations, these equations also allow one to calculate the  $\alpha$  angle of the transition moment associated with each vibration.

To verify the validity of eqs 14–16, they have been rearranged assuming a uniaxial orientation (i.e., a random distribution of the azimuthal angle ( $\varphi$ )). Integration was thus performed over this angle, causing  $f_\varphi$  to become equal to 0. Equations 14–16 then become

$$k_x = k_y = k_{\max} \left[ \frac{f_\theta \sin^2\alpha}{2} + \frac{1 - f_\theta}{3} \right] \quad (17)$$

$$k_z = k_{\max} \left[ \left( \cos^2\alpha - \left( \frac{1}{3} \right) \right) f_\theta + \left( \frac{1}{3} \right) \right] = k_{\max} \left[ f_\theta \cos^2\alpha + \frac{1 - f_\theta}{3} \right] \quad (18)$$

and are identical to those proposed by Fraser and McRae.<sup>40</sup>

## Materials and Methods

**Langmuir–Blodgett Deposition.** Poly(L-lactide) and poly(D-lactide) (PLLA and PDLA) were synthesized by ring-opening polymerization in toluene.<sup>44</sup> The molecular weight ( $M_w$ ) was  $1.32 \times 10^4$  g/mol for poly(L-lactide) (PLLA) and  $1.45 \times 10^4$  g/mol for poly(D-lactide) (PDLA), with a polydispersity index of 1.35 for both products.<sup>44</sup> PDLA and PLLA were dissolved in HPLC-grade chloroform (Sigma-Aldrich, St. Louis, MO) to a concentration of 0.1 mg/mL, and equal amounts of each solution were mixed to obtain a solution of the equimolar blend. Langmuir films were formed on a deionized water subphase (Barnstead International, Boston, MA) at  $35 \pm 1$  °C by spreading 160  $\mu$ L of the polylactide mixture. The Langmuir–Blodgett depositions were performed using a KSV 3000 apparatus (KSV Instruments, Helsinki, Finland) equipped with a  $80 \times 500$  mm<sup>2</sup> trough. After an equilibrating period of 15 min allowing solvent evaporation, the monolayers were com-

pressed at a rate of  $0.36 \text{ \AA}^2 (\text{repeat unit})^{-1} \text{ min}^{-1}$  until a surface pressure of 15 mN/m was reached. The film was held at this pressure for 15 min, and then the solid substrate that had been immersed in the subphase prior to the spreading was drawn from the subphase at a rate of 0.5 mm/min. Monolayers have been deposited on calcium fluoride windows and gold mirrors that had been thoroughly cleaned prior to deposition.

**FTIR Measurements.** Transmittance at normal and oblique incidence (incidence angle of 45°) and reflection–absorption (incidence angle of 75°) infrared spectra were recorded using a Magna 760 FTIR spectrometer (Thermo-Nicolet, Madison, WI) equipped with an MCT detector. A motorized rotating ZnSe wire-grid polarizer (Specac, Orpington, U.K.) was positioned in front of the sample to obtain parallel (p) and perpendicular (s) polarized spectra without breaking the purge of the spectrometer. All spectra were recorded by co-adding 1000 scans at a resolution of  $4 \text{ cm}^{-1}$  with two levels of zero filling.

Polarization modulation infrared reflection–absorption (PM-IRRAS) spectra of monolayers at the air/water interface were recorded using a Magna 850 spectrometer (Thermo-Nicolet, Madison, WI). The PM-IRRAS setup has been described in detail elsewhere.<sup>45</sup> The monolayers were formed by spreading 70  $\mu$ L of the polylactide mixture on a  $360 \times 50$  mm<sup>2</sup> homebuilt Langmuir trough. The polarized IR beam was focused on the water surface with an incidence angle of 70° (which is higher than the Brewster angle of the air/water interface (53.1°)) and was reflected by the water on a photovoltaic MCT detector (Kolmar Technologies, Newburyport). Prior to reflection on the water subphase, the initial p polarization of the IR beam was modulated with a photoelastic modulator (Hinds Instruments, type II) that was set for optimum efficiency at  $1450 \text{ cm}^{-1}$ . All spectra were recorded at a resolution of  $8 \text{ cm}^{-1}$  by co-adding 1000 scans. PM-IRRAS spectra are presented as normalized difference spectra  $(S(d) - S(0))/S(0)$ , where  $S(d)$  and  $S(0)$  are the spectra of the monolayer covered and uncovered water surfaces, respectively.

**Determination of the Anisotropic Optical Constants.** The anisotropic optical constants (i.e., the real ( $n$ , refractive index) and imaginary ( $k$ , extinction coefficient) parts of the complex refractive index) of multilayers of poly( $\gamma$ -benzyl-L-glutamate) (PBG) used for the calculation of the molecular orientation were those recently determined by Buffeteau et al.<sup>1</sup> The optical constants of the polylactides monolayer in the three direction of the space coordinate system were calculated using an iterative procedure based on the inversion of spectral simulation programs. Details of this procedure are given elsewhere.<sup>1,34</sup> The optical constants in the plane of the film ( $n_x$ ,  $k_x$  and  $n_y$ ,  $k_y$ ) were determined from p- and s-polarized transmittance spectra at normal incidence of the film deposited on a calcium fluoride window ( $n = 1.4$ ,  $k = 0$ ).<sup>46</sup> Indeed, for transmittance spectra recorded at normal incidence, the electric vector of the infrared radiation is in the surface plane, and only the ( $x$ ,  $y$ ) components of the transition moment can be observed. The out-of-plane optical constants ( $n_z$ ,  $k_z$ ) were determined from a p-polarized IRRAS spectrum of the thin film deposited on a gold mirror ( $n = 3$ ,  $k = 30$ ).<sup>47</sup> In this case, the electric vector is nearly perpendicular to the surface and interacts almost exclusively with the normal component ( $z$ ) of the transition moments of molecules. The determination of the spectral dependence of the optical constants of the polylactide monolayer ( $n_x$ ,  $n_y$ ,  $n_z$ ,  $k_x$ ,  $k_y$ , and  $k_z$ ) was performed using an  $n_\infty$  value (refraction index in the visible) of 1.47<sup>48</sup> and an estimated film thickness of 15  $\text{\AA}$ . Although this estimated film thickness does not allow the determination of the absolute values of  $n$  and  $k$ , it nevertheless



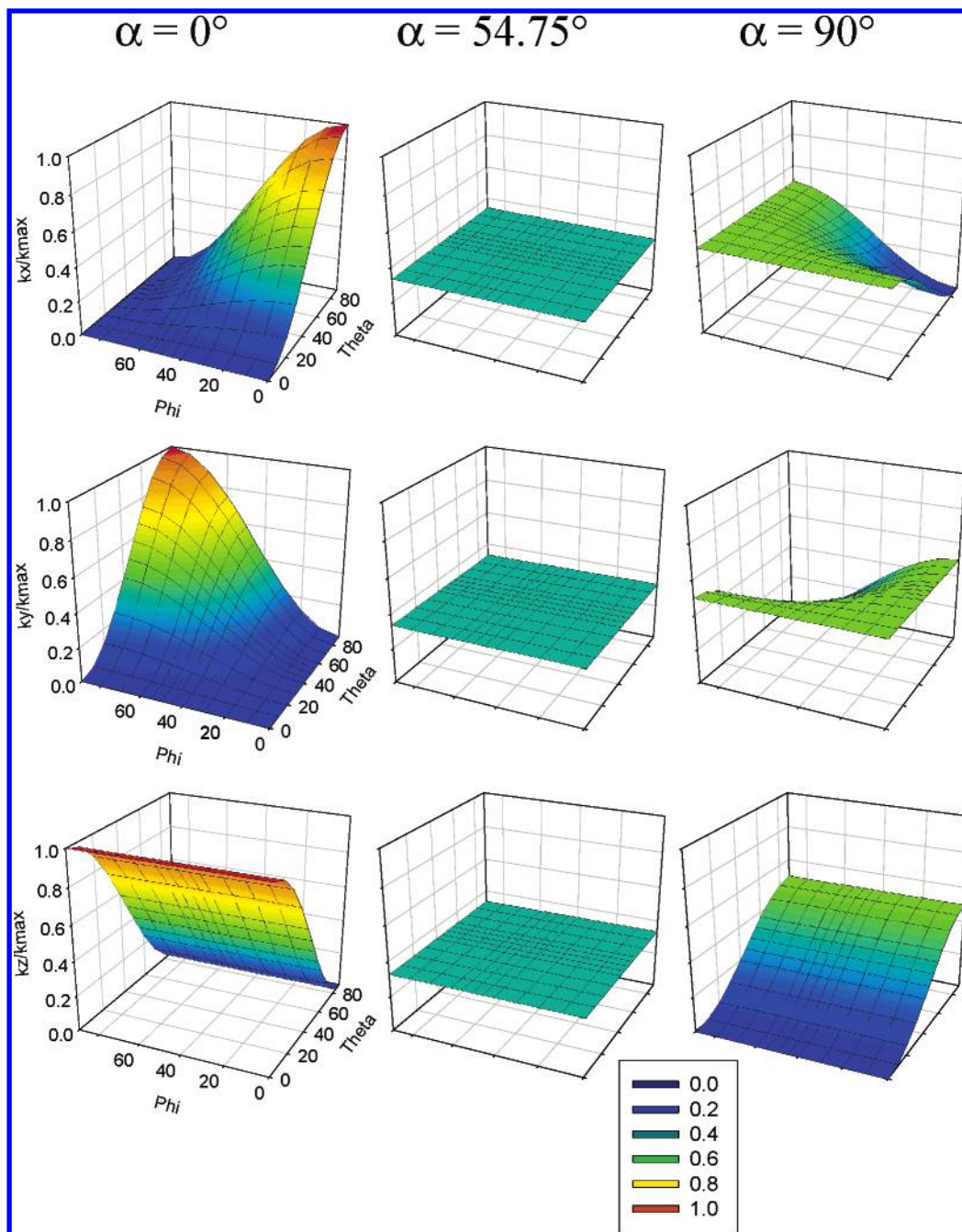


**Figure 1.** Variation of  $k_x/k_{\max}$ ,  $k_y/k_{\max}$ , and  $k_z/k_{\max}$  with  $\theta$  and  $\phi$  for  $\alpha$  values of 0, 54.75, and  $90^\circ$ .

allows precise calculations of the molecular orientation because this parameter depends only on the relative values of  $k_x$ ,  $k_y$ , and  $k_z$ .

**Calculation of  $\varphi$  and  $\theta$  Using the Optical Constants.** Once the optical constants were determined, the  $k_{\max}$  of each band was calculated by summing its  $k_x$ ,  $k_y$ , and  $k_z$  values. An iterative procedure was then used to determine the molecular orientation ( $\theta$  and  $\varphi$  angles) from these values. In this procedure, the  $k_{\max}$ , the  $\alpha$  angle (or at least a good estimation from the literature), and initial values of  $\theta$  and  $\varphi$  ( $45^\circ$ ) were introduced in eqs 14–16 to obtain the first set of calculated  $k_x$ ,  $k_y$ , and  $k_z$  values for each band. Then, the squared difference between these values and those determined using the infrared spectra was calculated for each band, and finally, the sum of these squared differences was minimized using the solver tool of Microsoft Excel. The  $\alpha$ ,  $\varphi$ , and  $\theta$  angles ( $\varphi$  and  $\theta$  were forced to be identical for all bands) were perturbed until the calculated  $k_x$ ,  $k_y$ , and  $k_z$  values

of each band were as close as possible to the values determined using the infrared spectra. The  $\alpha$  angle was fixed if only one band was available for the calculation.

## Results and Discussion

**Theoretical Calculation of  $k_x$ ,  $k_y$ , and  $k_z$ .** Using eqs 14 to 16, we calculated the values of  $k_x$ ,  $k_y$ , and  $k_z$  for a given value of  $k_{\max}$  for different ( $\theta$ ,  $\varphi$ ) couples (where  $\theta$  and  $\varphi$  vary between 0 and  $90^\circ$ ) and for  $\alpha$  values of 0, 54.75, and  $90^\circ$ . The variations of  $k_x/k_{\max}$ ,  $k_y/k_{\max}$ , and  $k_z/k_{\max}$  with  $\theta$  and  $\varphi$  for these  $\alpha$  angles are shown in Figure 1. This figure shows that the maximum and minimum possible values of  $k_x/k_{\max}$ ,  $k_y/k_{\max}$ , and  $k_z/k_{\max}$  are identical for a given  $\alpha$  angle but vary greatly for different values of  $\alpha$ . Indeed, for  $\alpha = 0^\circ$ ,  $k_x$ ,  $k_y$ , and  $k_z$  vary between 0 and 100% of  $k_{\max}$ , but they vary only from 0 to 50% of  $k_{\max}$  for  $\alpha = 90^\circ$ . Strikingly, for  $\alpha = 54.75^\circ$ ,  $k_x$ ,  $k_y$ , and  $k_z$  are very close to  $(1/3)k_{\max}$  for all ( $\theta$ ,  $\varphi$ ) couples. This is due to the fact that the

**TABLE 1: Values of  $k_x$ ,  $k_y$ , and  $k_z$  Obtained from the Infrared Spectra, Values of  $\alpha$  Obtained from the Literature, and Values of  $k_x$ ,  $k_y$ ,  $k_z$ , and  $\alpha$  Obtained Using the Iterative Procedure for PBG Multilayers**

band	values obtained from infrared spectra <sup>1</sup>			values obtained using the iterative procedure			$\alpha$ iter (deg)	$\alpha$ lit (deg)	ref
	$k_x$ ( $\pm 0.03$ )	$k_y$ ( $\pm 0.03$ )	$k_z$ ( $\pm 0.03$ )	$k_x$	$k_y$	$k_z$			
$\nu$ C=O	0.30	0.31	0.22	0.27	0.33	0.24	49	53	49
amide I	0.43	0.76	0.23	0.44	0.75	0.22	34	34–38	1
								39	49
								29–34	50
								38	51
amide II	0.23	0.13	0.31	0.23	0.13	0.31	74	76	1
								74–76	49
								75–77	50
								73	51

terms  $((1/2)\sin^2 \alpha - (1/3))$  and  $(\cos^2 \alpha - (1/3))$  in eqs 14–16 are equal to zero for this (so-called magic) angle. This means that a band having its transition moment at an angle around  $55^\circ$  of the molecular axis will always give rise to  $k_x$ ,  $k_y$ , and  $k_z$  values equal to  $(1/3)k_{\max}$  independently of  $\theta$  and  $\varphi$  and thus will be unusable to calculate the  $\theta$  and  $\varphi$  angles. Calculations of the molecular orientation from values of  $k_x$ ,  $k_y$ , and  $k_z$  obtained using eqs 14–16 have shown that  $\alpha$  angles between  $50$  and  $60^\circ$  are improper for the determination of molecular orientation.

**Biaxially Oriented Film with Molecular Cylindrical Symmetry: Poly( $\gamma$ -benzyl-L-glutamate).** Buffeteau et al.<sup>1</sup> have recently determined the anisotropic optical constants of multilayers of poly( $\gamma$ -benzyl-L-glutamate) (PBG). From these optical constants, they have determined the azimuthal angle  $\varphi$  and the angle  $\alpha$  between the transition moments of the amide I and amide II modes and the  $\alpha$ -helix axis, considering that  $\theta$  was equal to  $90^\circ$ . Here, the iterative procedure previously described has been used to calculate the molecular orientation in PBG multilayers from their optical constants, without making any assumption about the tilt angle of the helices. Three different bands of the infrared spectrum have been used for this calculation: the band due to the carbonyl stretching mode of the ester group ( $\nu$  C=O) and the amide I and II modes of the amide group. The initial  $\alpha$  angles for these bands were set equal to  $53$ ,  $39$ , and  $75^\circ$ , respectively.<sup>49</sup> These angles were then perturbed during the iterative procedure. Table 1 shows the values of  $k_x$ ,  $k_y$ , and  $k_z$  determined using the infrared spectra and the  $\alpha$  values from the literature along with the extinction coefficients and the  $\alpha$  angles obtained by the iterative procedure. All extinction coefficients obtained using this procedure are very close to those determined from the infrared spectra, proving that the iterative procedure has converged toward a valid solution. The  $\theta$  and  $\varphi$  angles calculated by this procedure are equal to  $89$  and  $57^\circ$ , respectively, and are in excellent agreement with those found by Buffeteau et al. ( $\theta = 90^\circ$ ,  $\varphi = 57^\circ$ )<sup>1</sup> and by Takenaka et al. ( $\theta = 90^\circ$ ,  $\varphi = 55^\circ$ ).<sup>28</sup>

To obtain the best agreement between the values of  $k_x$ ,  $k_y$ , and  $k_z$  obtained using the iterative procedure and those obtained from the spectra, the  $\alpha$  angle of each band has been varied during the iterative procedure. Because the initial values of  $\alpha$  found in the literature are supposed to be very good approximations of the real  $\alpha$  angles, the values obtained by the iterative procedure should be very close to these initial values. Indeed, for the amide I and II bands, the literature values<sup>1,49–51</sup> range from  $29$  to  $39^\circ$  and from  $74$  to  $77^\circ$ , respectively, and the calculated values of  $\alpha$  ( $34$  and  $74^\circ$  for the amide I and II bands, respectively) fall quite well within these ranges. However, for the  $\nu$  C=O band, the calculated  $\alpha$  angle ( $49^\circ$ ) is  $4^\circ$  smaller than the value reported by Tsuboi et al. ( $53^\circ$ ).<sup>49</sup>

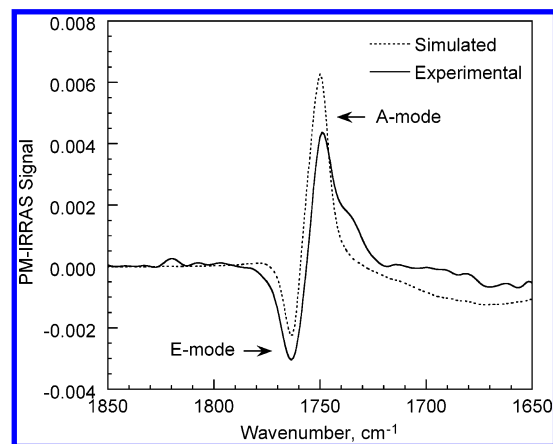


**Figure 2.** Experimental and simulated PM-IRRAS spectra of a Langmuir film of an equimolar polylactide mixture recorded at a surface pressure of 15 mN/m.

**Biaxially Oriented Film without Molecular Cylindrical Symmetry: Polylactides.** Poly(L-lactide) (PLLA) and poly(D-lactide) (PDLA) are helical optically active semicrystalline polymers that can form a racemic stereocomplex when their equimolar blend is crystallized from the melt or from solution.<sup>52</sup> Polarization-modulation infrared reflection–absorption spectroscopy (PM-IRRAS) has already been used to record infrared spectra of monolayers of the equimolar blend of PLLA and PDLA at the air/water interface.<sup>45</sup> This technique is particularly well suited for this purpose because, in addition to being unaffected by the isotropic absorptions of the sample environment, PM-IRRAS gives spectra in which the orientation of the bands with respect to the baseline is directly related to the orientation of the transition moments.<sup>53,54</sup> Indeed, in a PM-IRRAS spectrum, a positive band indicates that the transition moment of the associated vibration is preferentially oriented in the plane of the water subphase, whereas a negative band is indicative of a transition moment preferentially oriented perpendicular to the water subphase.

In the PM-IRRAS spectrum of the polylactide mixture monolayer, shown in Figure 2, the band due to the stretching mode of the carbonyl is clearly split into two components of opposite sign. The positive, low-frequency ( $1749\text{ cm}^{-1}$ ) component has been assigned to the A mode of the coupled carbonyl vibrations of the polylactide helices (with its transition moment parallel to the helix axis), and the negative, high-frequency ( $1763\text{ cm}^{-1}$ ) component has been assigned to the E mode of these vibrations (with its transition moment perpendicular to the helix axis).<sup>45,55,56</sup> For an isolated helix lying parallel to the water surface, the PM-IRRAS signal associated with the A mode (entirely in the plane of the water subphase) should be a strongly

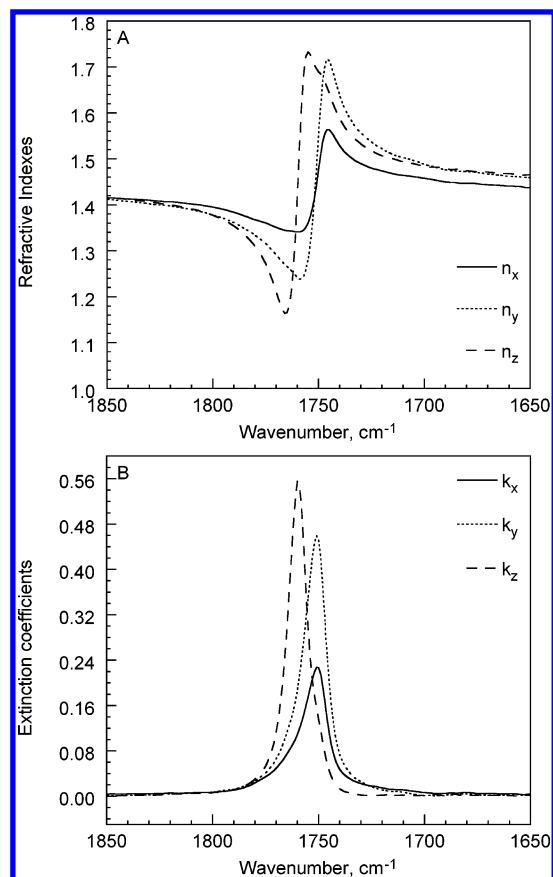


**Figure 3.** Anisotropic (A) refractive indexes and (B) extinction coefficients of a monolayer of an equimolar polylactide mixture.

positive band similar to that observed experimentally, and the signal associated with the doubly degenerate E mode (perpendicular to the helix axis and then oriented at  $45^\circ$  from the plane of the water subphase) should be a slightly positive band as opposed to the negative band observed in the experimental spectrum. Bourque et al. have suggested that an intermolecular coupling occurs between the polylactide helices in the plane of the film and results in the selective attenuation of the in-plane component of the E mode, leaving its out-of-plane component unaffected.<sup>45</sup> In this case, the transition moment associated with the E mode would be perpendicular to the plane of the film and would result in a negative PM-IRRAS band.

This in-plane attenuation of the E mode implies that this mode does not display cylindrical symmetry. In principle, eqs 14–16 cannot be used to calculate the molecular orientation in this case because they have been derived assuming cylindrical symmetry of the molecules around their main axis. Moreover, tests have shown that most of the other bands in the infrared spectrum of the polylactide mixture do not display cylindrical symmetry. Fortunately, the A mode of the carbonyl stretching vibration, which is parallel to the axis of the helix, presents intrinsic cylindrical symmetry that allows the calculation of the molecular orientation.

The anisotropic optical constants of the monolayer of the equimolar PDLA/PLLA mixture, shown in Figure 3A and B, were determined using p- and s-polarized transmittance and p-polarized IRRAS spectra of the monolayer deposited on calcium fluoride and on gold mirrors (results not shown). It is clear from Figure 3B that, in agreement with the model proposed by Bourque et al., the high-frequency E mode is very strong in the z direction but is almost entirely extinguished in the plane of the film. On the contrary, the A mode at lower frequency is

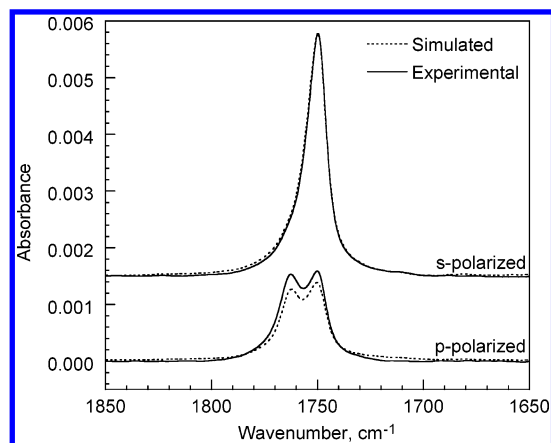


**Figure 4.** Experimental and simulated oblique incidence transmittance spectra of a monolayer of an equimolar polylactide mixture.

very weak in the z direction but is quite strong in the x and y directions. However, it is clear from the shape of the bands for the x and y extinction coefficients ( $k_x$  and  $k_y$ ) that the E mode is only partially extinguished in the plane of the film. Moreover, the extinction coefficient in the z direction has a shoulder that can be attributed to the A mode, indicating that the helices are not perfectly parallel to the plane of the film. The different values of  $k_x$  and  $k_y$  observed for the A mode indicate that the PLA helices also possess a preferential orientation in the plane of the film, confirming the biaxial orientation of this film.

The optical constants have been used to simulate the p- and s-polarized transmittance spectra of the polylactide mixture monolayer recorded at oblique incidence. The simulated and experimental spectra, shown in Figure 4, are almost identical, proving the validity of these optical constants. In the p-polarized spectrum that probes transition moments in the plane and out of the plane of the film, both the A and E modes are clearly visible. The s-polarized spectrum that probes only the transition moments in the plane of the film shows one peak, assigned to the A mode, with a very small shoulder attributed to the E mode. The calculated optical constants have also been used to simulate the PM-IRRAS spectrum of the polylactide mixture monolayer on a water surface. The simulated spectrum, shown in Figure 2, does not perfectly reproduce the experimental one. Indeed, the low-frequency band (A mode) in the experimental spectrum displays a shoulder on the low-frequency side that is not present in the simulated spectrum. This shoulder is most likely due to the stretching mode of carbonyl groups that are hydrogen bonded to water molecules in the Langmuir film. Nevertheless, the simulated spectrum clearly shows the positive, low-frequency A mode and the negative, high-frequency E mode, indicating that the helices adopt a similar orientation at the water surface and on solid substrates. This means that the molecular orientation found at the air/water interface would probably be similar to that calculated for films on solid substrates.

To determine the exact intensities of  $k_x$ ,  $k_y$ , and  $k_z$  for the A and E modes, the peaks appearing in Figure 3B have been decomposed into their components using the peak-fitting tool of Grams/AI 7.00 software. The  $k_x$ ,  $k_y$ ,  $k_z$  peaks have been fit, in Figure 5, with two bands located at positions corresponding to those observed for the C=O stretching band in the transmission and IRRAS spectra. Figure 5 shows very clearly that the E mode is not totally extinguished in the plane of the film and that the A mode, although very weak, is not totally absent in the z direction. The exact positions, intensities, widths at half-height, and percentages of Lorentzian shape of the A and E modes in the x, y, and z directions are given in Table 2 along



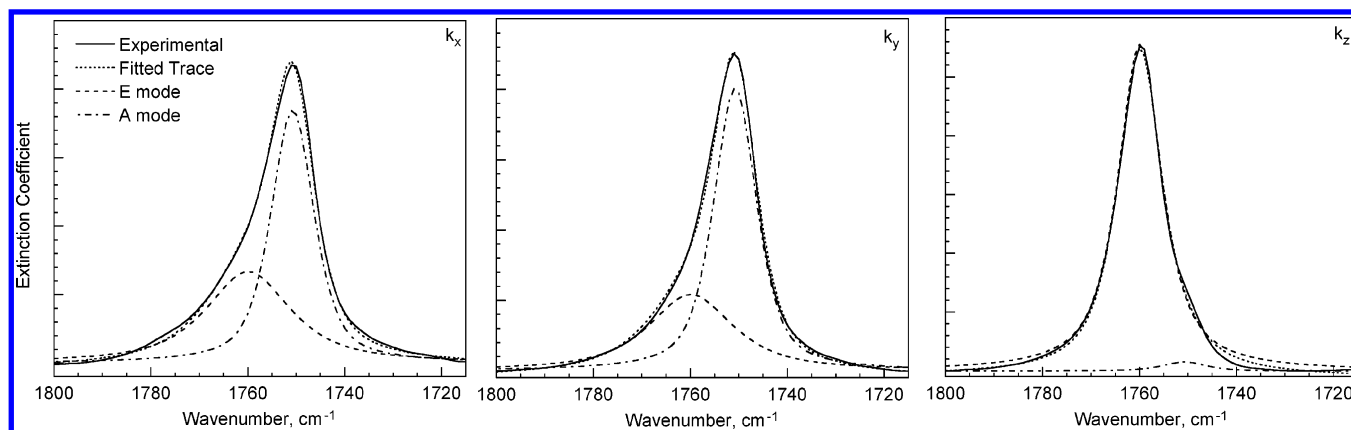


**Figure 5.** Spectral fit of the anisotropic extinction coefficients of a monolayer of an equimolar polylactide mixture.

**TABLE 2: Position, Height, Width at Half-Height, and Percentage of Lorentzian Shape of the A- and E-Mode Components of  $k_x$ ,  $k_y$ , and  $k_z$**

		$k_x$	$k_y$	$k_z$
E mode	position (cm <sup>-1</sup> )	1759.9	1759.9	1759.9
	height	0.067	0.108	0.555
	width (cm <sup>-1</sup> )	20.8	20.8	10.9
	% Lorentzian	80	80	80
A mode	position (cm <sup>-1</sup> )	1750.8	1750.8	1750.8
	height	0.185	0.401	0.015
	width (cm <sup>-1</sup> )	10.6	10.6	10.6
	% Lorentzian	59	59	59
correlation $R^2$		0.9983	0.9986	0.9982

**TABLE 3: Values of  $k_x$ ,  $k_y$ , and  $k_z$  Obtained from Infrared Spectra and Values Obtained from the Iterative Procedure for a PLA Monolayer**

	values obtained from the spectral fit			values obtained using the iterative procedure		
	$k_x$	$k_y$	$k_z$	$k_x$	$k_y$	$k_z$
A mode	0.185	0.401	0.015	0.185	0.401	0.015
E mode	0.067	0.108	0.555	0.162	0.204	0.365
E mode ( $\alpha = 0^\circ$ )	0.067	0.108	0.555	0.067	0.108	0.555

the correlation coefficients ( $R^2$ ) obtained for the fits. In this table, it is clear that the E mode is broader in the  $x$  and  $y$  directions. This broadening is most likely due to the intermolecular coupling that occurs between the polylactide helices and that attenuates the E mode in the ( $x$ ,  $y$ ) plane.

Using the  $k_x$ ,  $k_y$ , and  $k_z$  values found by the spectral fit for the A and E modes and fixed  $\alpha$  angles of 0 and 90° for these modes, respectively, we have calculated the molecular orientation of the polylactide helices using the iterative procedure previously described. For the A mode, the values of  $k_x$ ,  $k_y$ , and  $k_z$  obtained with this procedure, shown in Table 3, perfectly fit the values calculated by the spectral fit, demonstrating the convergence of the iterative procedure. Values of 81 and 56° have been calculated for  $\theta$  and  $\varphi$ , respectively. These values reflect the fact that, on solid substrates, the polylactide helices are not perfectly parallel to the plane of the film, in contrast to the PBG helices, and that they have a preferential orientation in the plane of the film similar to that of PBG. Indeed, the helices are preferentially oriented parallel to the drawing direction of the solid substrates during the LB deposition, in agreement with the observation of Schwiegk et al.<sup>12</sup> for monolayers of hairy-rod-type polymers.

For the E mode, which is perpendicular to the axis of the helix, the values of  $k_x$ ,  $k_y$ , and  $k_z$  obtained from the iterative procedure do not reproduce the values obtained with the spectral fit if the  $\alpha$  angle is fixed to 90°. (See Table 3, second row.)

This proves the noncylindrical symmetry of this mode around the helix axis, thus confirming the partial extinction of this mode in the plane of the film as proposed by Bourque et al.<sup>45</sup> Although the orientation of the helix cannot be calculated from the E mode, its  $k_x$ ,  $k_y$ , and  $k_z$  values can be used to calculate the orientation of the transition moment of this mode. Indeed, by fixing  $\alpha = 0^\circ$  prior to the iterative procedure, the calculated  $\theta$  and  $\varphi$  values will reflect the orientation of the transition moment with regard to the space coordinate system. The values of  $k_x$ ,  $k_y$ , and  $k_z$  obtained with this method, reported in the last row of Table 3, reproduce very well the values calculated with the spectral fit, and  $\theta$  and  $\varphi$  angles of 29 and 52° have been calculated. If the E mode had been totally extinguished in the plane of the film, then the calculated  $\theta$  angle would have been equal to 0°. The non-null  $\theta$  value obtained here confirms the non-total extinction of the mode in the plane of the film.

## Conclusions

In this paper, analytical expressions linking the optical constants (in the space coordinate system) of a biaxially oriented film with the molecular tilt and azimuthal angles ( $\theta$  and  $\varphi$ ) have been presented for the first time. These equations have been used to calculate the molecular orientation in multilayers of poly( $\gamma$ -benzyl-L-glutamate) (PBG). The calculated  $\theta$  and  $\varphi$  angles of this film are very close to those found in the literature, proving the validity of the new equations presented in this article.

The optical constants of a LB monolayer of an equimolar blend of poly(D-lactide) and poly(L-lactide) have also been determined. Except for the A mode of the carbonyl stretching vibration, none of the vibrations observed for this biaxially oriented film has cylindrical symmetry around the helix axis. Although the expressions presented here are valid only for transition moments showing such symmetry, we have been able, using the A mode, to calculate the molecular orientation in this film ( $\theta = 81^\circ$  and  $\varphi = 56^\circ$ ). We also observed the attenuation of the E mode of the amide I vibration in the plane of the film, confirming the hypothesis of Bourque et al. about the cause of the unusual shape observed in the PM-IRRAS spectrum of this film at the air/water interface.<sup>45</sup>

**Acknowledgment.** This work was supported by the Natural Sciences and Engineering Research Council of Canada (NSERC) and by the Fond québécois de la recherche sur la nature et les technologies (FQRNT). I.P. is also grateful to the NSERC and the FQRNT for postgraduate scholarships.

## References and Notes

- (1) Buffeteau, T.; Le Calvez, E.; Castano, S.; Desbat, B.; Blaudez, D.; Dufourcq, J. *J. Phys. Chem. B* **2000**, 4537.
- (2) Honeybourne, C. T. *Chem. Solids* **1987**, 48, 109.
- (3) Moriizumi, T. *Thin Solid Films* **1987**, 152, 345.
- (4) Seto, J.; Nagai, T.; Ishimoto, C.; Watanabe, N. *Thin Solid Films* **1985**, 134, 101.
- (5) West, R.; David, L. D.; Djurovitch, P. I.; Stearley, K. L.; Srinivasan, K. S. V.; Yu, H. J. *J. Am. Chem. Soc.* **1981**, 103, 1352.
- (6) Tredgold, R. H.; Young, M. C. J.; Hodge, P.; Khoshdel, E. *Thin Solid Films* **1987**, 151, 441.
- (7) Kani, R.; Yoshida, H.; Nakano, Y.; Murai, S.; Mori, Y.; Kawata, Y.; Hayase, S. *Langmuir* **1993**, 9, 3045.
- (8) Kani, R.; Nakano, Y.; Majima, Y.; Hayase, S.; West, R. *Macromolecules* **1994**, 27, 1911.
- (9) Okahata, Y.; Kobayashi, T.; Tanaka, K. *Langmuir* **1996**, 12, 1326.
- (10) Tachibana, H.; Kishida, H.; Tokura, Y. *Langmuir* **2001**, 17, 437.
- (11) Minari, N.; Ikegami, K.; Kuroda, S.; Saito, K.; Saito, M.; Sugi, M. *Solid State Commun.* **1988**, 65, 1259.
- (12) Schwiegk, S.; Vahlenkamp, T.; Xu, Y.; Wegner, G. *Macromolecules* **1992**, 25, 2514.
- (13) Mingotaud, C.; Agricole, B.; Jegou, C. *J. Phys. Chem. B* **1995**, 99, 17068.
- (14) Ikegami, K.; Mingotaud, C.; Delhaes, P. *Phys. Rev. E* **1997**, 56, 1987.
- (15) Chollet, P.-A.; Messier, J.; Rosilio, C. *J. Chem. Phys.* **1976**, 64, 1042.
- (16) Chollet, P.-A. *Thin Solid Films* **1978**, 52, 343.
- (17) Rabolt, J. F.; Burns, F. C.; Schlottter, N. E.; Swalen, J. D. *J. Chem. Phys.* **1983**, 78, 946.
- (18) Umemura, J.; Kamata, T.; Kawai, T.; Takenaka, T. *J. Phys. Chem.* **1990**, 94, 62.
- (19) Takenaka, T.; Umemura, J.; Kamata, T.; Kawai, T.; Koizumi, N. *Polym. J.* **1991**, 23, 357.
- (20) Hasegawa, T.; Umemura, J.; Takenaka, T. *J. Phys. Chem.* **1993**, 97, 9009.
- (21) Hasegawa, T.; Takeda, S.; Kawaguchi, A.; Umemura, J. *Langmuir* **1995**, 11, 1236.
- (22) Citra, M. J.; Axelsen, P. H. *Biophys. J.* **1996**, 71, 1796.
- (23) Axelsen, P. H.; Citra, M. J. *Prog. Biophys. Mol. Biol.* **1996**, 66, 227.
- (24) Hui-Litwin, H.; Servant, L.; Dignam, M. J.; Moskovits, M. *Langmuir* **1997**, 13, 7211.
- (25) Goormaghtigh, E.; Raussens, V.; Ruyschaert, J.-M. *Biochim. Biophys. Acta* **1999**, 1422, 105.
- (26) Hasegawa, T.; Nishijo, J.; Umemura, J.; Theiss, W. *J. Phys. Chem. B* **2001**, 105, 11178.
- (27) Hasegawa, T. *J. Phys. Chem. B* **2002**, 106, 4112.
- (28) Takenaka, T.; Harada, K.; Matsumoto, M. *J. Colloid. Interface Sci.* **1980**, 73, 569.
- (29) Takeda, F.; Matsumoto, M.; Takenaka, T.; Fujiyoshi, Y. *J. Colloid. Interface Sci.* **1981**, 84, 220.
- (30) Ahn, D. J.; Franes, E. I. *J. Phys. Chem.* **1992**, 96, 9952.
- (31) Ahn, D. J.; Franes, E. I. *Thin Solid Films* **1994**, 244, 971.
- (32) Marsh, D. *Biophys. J.* **1997**, 72, 2710.
- (33) Chernyshova, I. V.; Rao, K. H. *J. Phys. Chem. B* **2001**, 105, 810.
- (34) Buffeteau, T.; Blaudez, D.; Péré, E.; Desbat, B. *J. Phys. Chem. B* **1999**, 103, 5020.
- (35) Buffeteau, T.; Desbat, B.; Péré, E.; Turlet, J. M. *Mikrochim. Acta* **1997**, 14, 631.
- (36) Picard, F.; Buffeteau, T.; Desbat, B.; Auger, M.; Pézolet, M. *Biophys. J.* **1999**, 76, 539.
- (37) Blaudez, D.; Boucher, F.; Buffeteau, T.; Desbat, B.; Grandbois, M.; Salesse, C. *Appl. Spectrosc.* **1999**, 53, 1299.
- (38) Buffeteau, T.; Calvez, E. L.; Desbat, B.; Pelletier, I.; Pézolet, M. *J. Phys. Chem. B* **2001**, 105, 1464.
- (39) Pelletier, I.; Bourque, H.; Buffeteau, T.; Blaudez, D.; Desbat, B.; Pézolet, M. *J. Phys. Chem. B* **2002**, 106, 1968.
- (40) Fraser, R. D. B.; MacRae, T. P. *Conformation in Fibrous Proteins and Related Synthetic Polypeptides*; Academic Press: New York, 1973.
- (41) Zbinden, R. *Infrared Spectroscopy of High Polymers*; Academic Press: New York, 1964.
- (42) Stein, R. S. *J. Polym. Sci.* **1961**, 31, 327.
- (43) Stein, R. S. *Newer Methods of Polymer Characterization*; Wiley-Interscience: New York, 1964.
- (44) Brochu, S.; Prud'homme, R. E.; Barakat, I.; Jérôme, R. *Macromolecules* **1995**, 28, 5230.
- (45) Bourque, H.; Laurin, I.; Pézolet, M.; Klass, J. M.; Lennox, R. B.; Brown, G. R. *Langmuir* **2001**, 17, 5842.
- (46) *American Institute of Physics Handbook*; Gray, D. E., Ed.; McGraw-Hill: New York, 1972.
- (47) *Handbook of Optical Constants of Solids*; Palik, E. D., Ed.; Academic Press: Boston, 1985.
- (48) Bartus, J.; Weng, D.; Vogl, O. *Polym. Int.* **1994**, 34, 433.
- (49) Tsuboi, M. *J. Polym. Sci.* **1962**, 59, 139.
- (50) Miyazawa, T.; Blout, E. R. *J. Am. Chem. Soc.* **1961**, 83, 712.
- (51) Marsh, D.; Müller, M.; J. Schmitt, F. *Biophys. J.* **2000**, 78, 2499.
- (52) Ikada, Y.; Jamashidi, K.; Tsuji, H.; Hyon, S.-H. *Macromolecules* **1987**, 20, 904.
- (53) Blaudez, D.; Buffeteau, T.; Cornut, J. C.; Desbat, B.; Escafre, N.; Pézolet, M.; Turlet, J.-M. *Appl. Spectrosc.* **1993**, 47, 869.
- (54) Blaudez, D.; Buffeteau, T.; Cornut, J. C.; Desbat, B.; Escafre, N.; Pézolet, M.; Turlet, J.-M. *Thin Solid Films* **1994**, 242, 146.
- (55) Kister, G.; Cassanas, G.; Vert, M. *Polymer* **1998**, 39, 267.
- (56) Klass, J. M.; Lennox, R. B.; Brown, F. R.; Bourque, H.; Pézolet, M. *Langmuir* **2003**, 19, 333.